Electronic supporting information for:

Metal-organic frameworks combined with mid-infrared spectroscopy for the trace analysis of phosphates in water

Felix Frank, Bettina Baumgartner, and Bernhard Lendl

S1) Further characterisation of NH_2-MIL-88B(Fe)

To demonstrate the successful synthesis of the NH_2-MIL-88B(Fe) as a crystalline MOF, scanning electron microscopy (SEM) was performed. For that, the MOF was suspended in IPA with a concentration of 0.03 wt% and stirred for 1 h. The suspension was then drop-casted on a silicon wafer and mounted on the SEM sample holder. For better contrast, the sample was sputter-coated with a 20 nm layer of Au. The SEM images seen in Figure S1 were recorded in secondary electron configuration on a FEI QUANTA 200 ESEM scanning electron microscope at magnifications of 30,000x and 160,000x. In the image acquired at 30,000x, the tendency of the MOF to form aggregates can be seen clearly, with some aggregates with a size of > 3 µm forming. However, most of the aggregates can be broken up by stirring, as seen by the presence of the small octahedral crystals (with a size of around 400 nm as seen in the right image at 160,000x magnification).

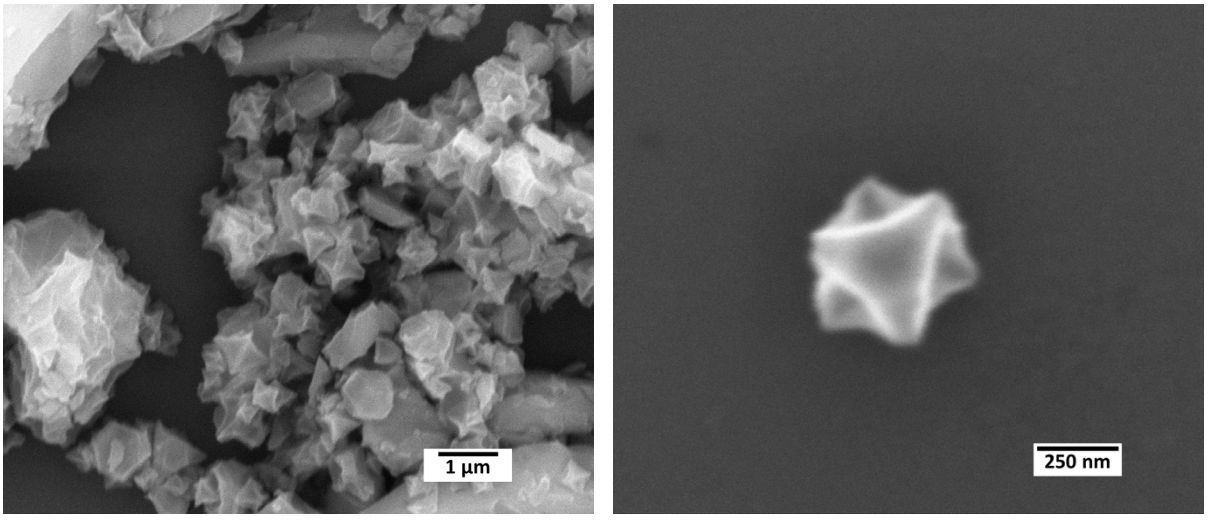

Figure S1: Scanning electron microscopy images of isolated NH_2-MIL-88B(Fe) crystals with magnifications of 30,000x (left) and 160,000x (right).

Additionally, nitrogen adsorption-desorption experiments were performed to give additional information on the porous nature of the MOF. The isotherm is shown in Figure S2 and shows a type I isotherm, which hints to microporosity being present in the MOF. This seems to be supported by the BHJ pore size distribution, with a peak of differential pore volume present below 2 nm. [1]

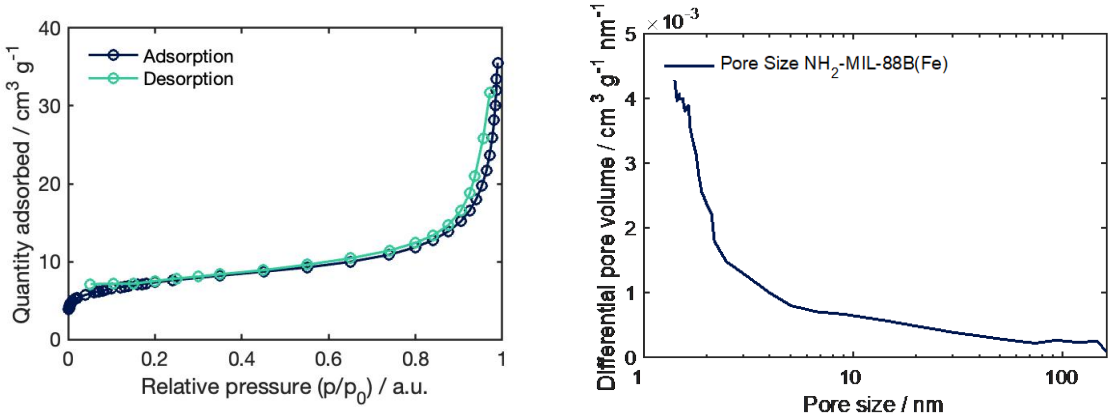

Figure S2: Results of the nitrogen adsorption-desorption experiments performed with the used NH_2-MIL-88B(Fe) MOF.

To check the thermal stability of the synthesised MOF, a thermogravimetric (TG) study was performed. The results of this study are shown in Figure S3. Looking at the course of the thermal-induced mass loss, three regions of mass losses can be seen: After the loss of adsorbed solvents and water, which happens linearly, accounting to a loss of approximately 8 %, the first onset starts at 250 °C, following a mass loss of 14 %. The second onset starts at 350°C, following a mass loss of 24 %. Finally, the third mass loss starts at 540 °C, accompanied by another mass loss of 10 %. Due to the absence of plateaus, it is impossible to explain the exact processes causing these mass losses, however the mass loss of 14 % may account for a partial decomposition of non-coordinating ligands, followed by decomposition of the MOF structure and decomposition of the remaining ligands. Regardless of this, the TG study confirms the thermal stability of the NH_2-MIL-88B(Fe) MOF at temperatures below 250 °C.[2]

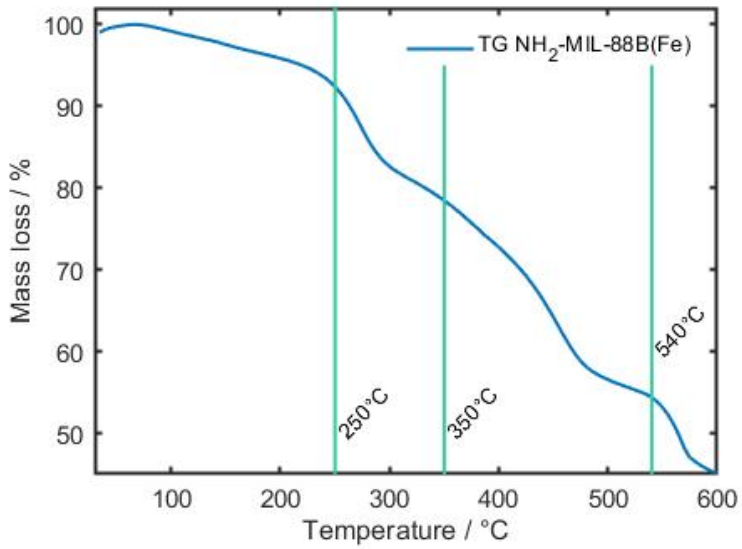

Figure S3: Results of the thermogravimetry of the used NH_2-MIL-88B(Fe) MOF.

S2) Experiments involving Fe_2O_3 MP enrichment layers

To assess the influence of the porosity of the MOF, comparative phosphate enrichment experiments with Fe_2O_3 MPs were performed. Fe_2O_3 particles with similar particle size to the synthesized MOF were employed as it can be seen in the light microscopy images in Figure S4.

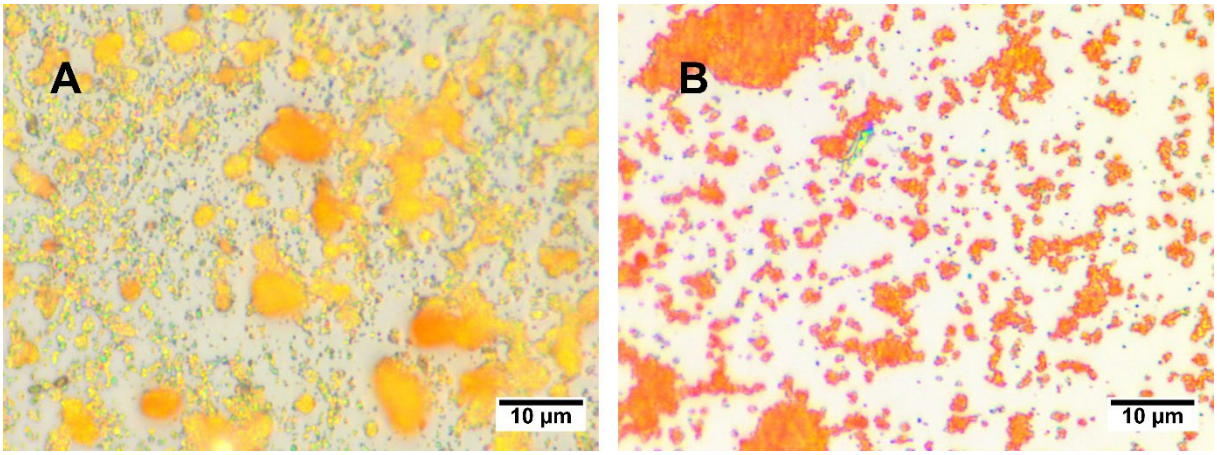

Figure S4: Light microscopy images of coated NH_2-MIL-88B(Fe) (A) and Fe_2O_3 (B) layers.

For the enrichment experiments, two adjustments were made, addressing the significantly lower phosphate loading capacity of the Fe_2O_3 MPs:

1. In the SIA sequence, no reference concentration was applied, as this obstructed the sample measurements to the point that no detection of phosphate was possible.
2. Instead of the concentration series of 5-75 mg L^{-1}, higher concentrations up to 200 mg L^{-1} phosphate were applied.

In Figure S5, spectra of the enriched phosphates on the two respective enrichment layers are shown, showing 10-20 times reduced enrichment of the Fe_2O_3 MPs as compared to the MOF.

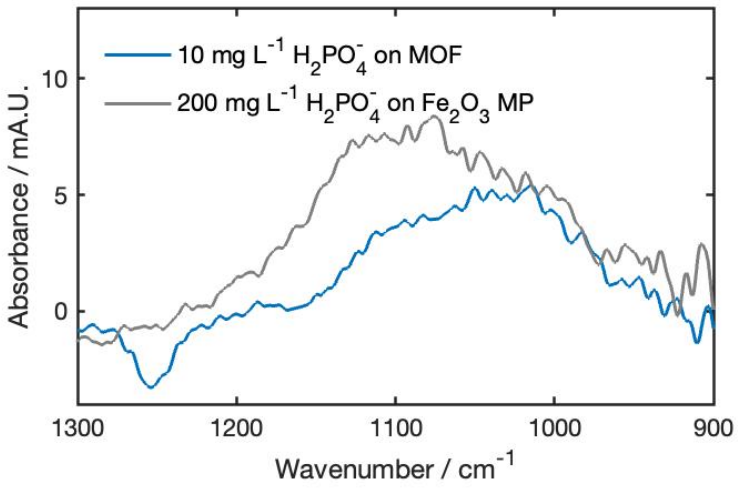

Figure S5: Spectra of the enriched phosphate on the two respective model layers, NH_2-MIL-88B(Fe) (10 mg L^{-1} phosphate, blue) and the Fe_2O_3 MP (200 mg L^{-1} phosphate, grey)

S3) Characterising the SIA system with a phosphate tracer solution

The volume of the used aluminium flow cell was 20 µL. Added to that, a dead volume of 78 µL (50 cm of Teflon tubing with an I.D. of 0.5 mm) equates to a total volume of 98 µL needed to be displaced by the sample solution. Thus, 300 µL (roughly three times the total volume) was chosen for the sample pulse. To verify whether the whole volume was exchanged by only one pulse, calibration experiments with phosphate tracer solutions (150 – 1000 mg L^{-1}) using the uncoated ATR crystal were performed. For the calibration, the strongest absorption band at 1077 cm^{-1} was taken, leading to almost identical calibration functions as seen in Figure S6.

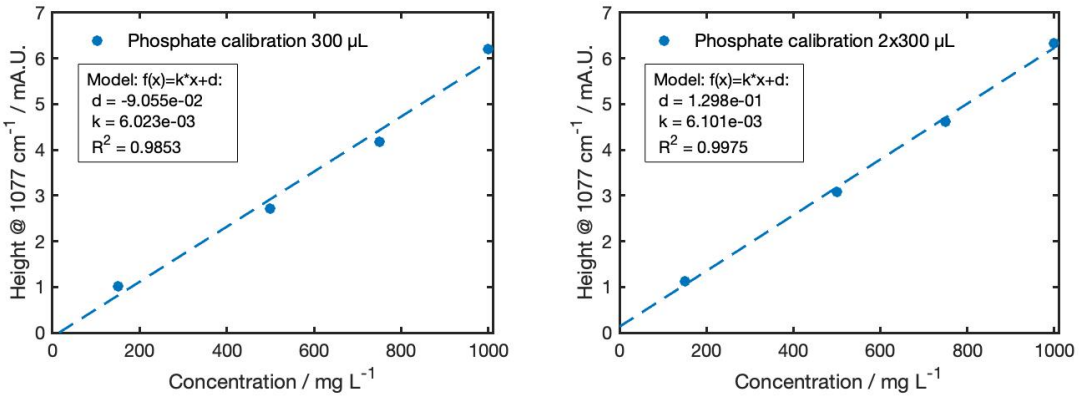

Figure S6: Comparison of the calibration functions of phosphate solutions applying one pulse (300 µL, left) and two pulses (2x300 µL, right) using the same flow cell setup.

S4) Comparison of different data analysis schemes

The referenced experimental adsorption data were fitted with Langmuir and Freundlich isotherms, with the two obtained calibrations shown in Figure S7. The χ^2 values of the Langmuir model (0.0300) were lower than those of the Freundlich (0.0619) model, indicating a better fit for this isotherm.

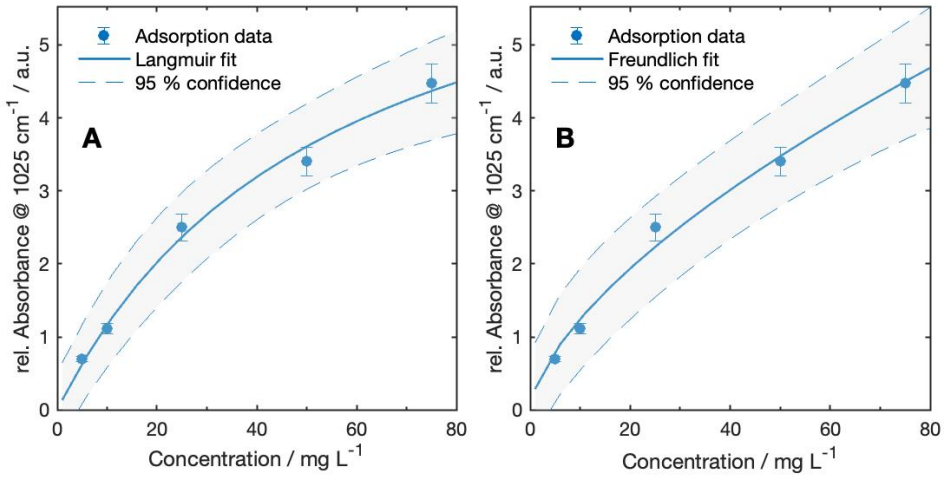

Figure S7: Comparison of data fitted with the Langmuir equation (A) and data fitted with the Freundlich equation. The band height was referenced to the reference concentration of 10 mg L^{-1}. Error bars show the standard deviation for each concentration (n = 3 for each respective concentration). Data points were fitted with the respective equations (solid lines) with a 95 % confidence of the fit (dashed lines).

The SIA scheme was designed to account for variance in phosphate intake caused by differences in the spin-coated enrichment layer by implementing a reference step. The necessity of this and the associated single point calibration is apparent when comparing the relative errors of the non-referenced data to the relative errors of the referenced data in Figure S8. While the relative errors for the referenced data lie between 5.0 % and 6.2 % (repeatability of 94 %), the relative errors of the non-referenced data lie between 19.3 % and 22.6 % for the concentrations between 10 mg L^{-1} and 75 mg L^{-1}, and even close to 40 % for the lower concentration of 5 mg L^{-1} (repeatability of 74 %). These high

relative errors for the non-referenced data stem from the variance in phosphate intake caused by differences in the spin-coated enrichment layer.

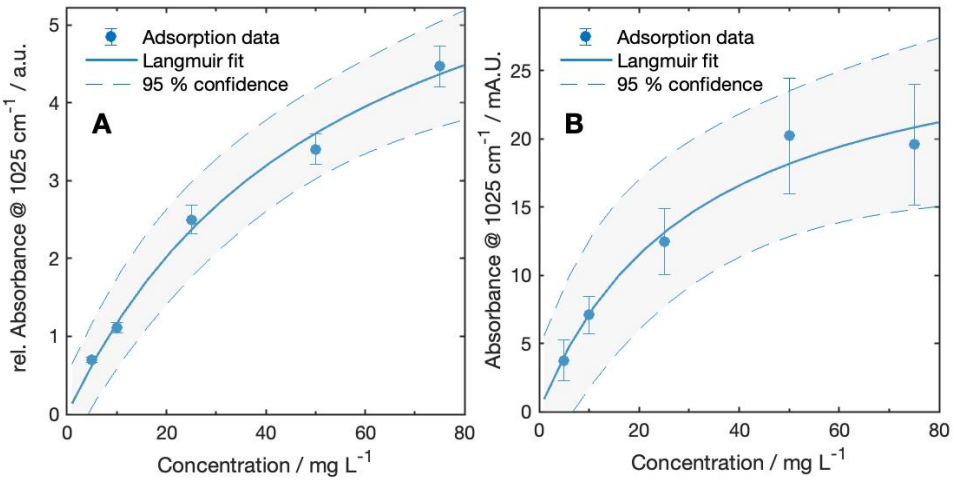

Figure S8: Comparison of referenced phosphate band heights as function of the applied concentration (A) to the unreferenced phosphate band heights as function of the applied concentration. The band height was referenced to the reference concentration of 10 mg L^{-1}. Error bars show the standard deviation for each concentration (n = 3 for each respective concentration). Data points were fitted with the Langmuir equation (solid lines) with a 95 % confidence of the fit (dashed lines).

References

[1] H. Guo, B. Niu, X. Wu, Y. Zhang, S. Ying, Effective removal of 2,4,6-trinitrophenol over hexagonal metal–organic framework NH2-MIL-88B(Fe), Appl. Organometal. Chem. 33 (2019) e4580. https://doi.org/10.1002/aoc.4580.
[2] Z.U. Zango, K. Jumbri, N.S. Sambudi, N.H. Hanif Abu Bakar, N.A. Fathihah Abdullah, C. Basheer, B. Saad, Removal of anthracene in water by MIL-88(Fe), NH2-MIL-88(Fe), and mixed-MIL-88(Fe) metal–organic frameworks, RSC Adv. 9 (2019) 41490-41501. https://doi.org/10.1039/C9RA08660A.